LBL-12895 c.2
Preprint

Lawrence Berkeley Laboratory

UNIVERSITY OF CALIFORNIA

Materials & Molecular Research Division

RECEIVED
LAWRENCE
BERKELEY LABORATORY
JUL 17 1981
LIBRARY AND
DOCUMENTS SECTION

Submitted to the Journal of Physical Chemistry

VIBRATIONAL PREDISSOCIATION OF BENZENE DIMERS AND TRIMERS BY THE CROSSED LASER-MOLECULAR BEAM TECHNIQUE

M.F. Vernon, J.M. Lisy, H.S. Kwok, D.J. Krajnovich, A. Tramer, Y.R. Shen, and Y.T. Lee

June 1981

TWO-WEEK LOAN COPY

This is a Library Circulating Copy which may be borrowed for two weeks. For a personal retention copy, call Tech. Info. Division, Ext. 6782.

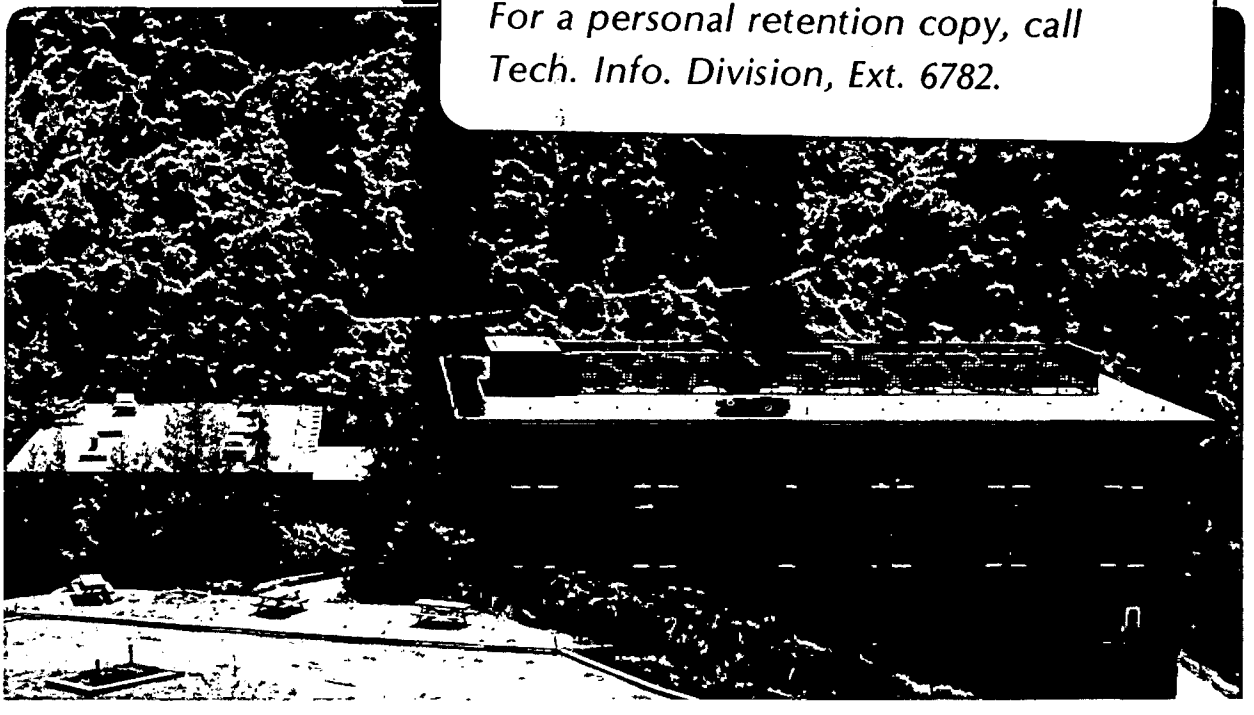

Prepared for the U.S. Department of Energy under Contract W-7405-ENG-48

LBL-12895 c.2

DISCLAIMER

This document was prepared as an account of work sponsored by the United States Government. While this document is believed to contain correct information, neither the United States Government nor any agency thereof, nor the Regents of the University of California, nor any of their employees, makes any warranty, express or implied, or assumes any legal responsibility for the accuracy, completeness, or usefulness of any information, apparatus, product, or process disclosed, or represents that its use would not infringe privately owned rights. Reference herein to any specific commercial product, process, or service by its trade name, trademark, manufacturer, or otherwise, does not necessarily constitute or imply its endorsement, recommendation, or favoring by the United States Government or any agency thereof, or the Regents of the University of California. The views and opinions of authors expressed herein do not necessarily state or reflect those of the United States Government or any agency thereof or the Regents of the University of California.

LBL-12895

VIBRATIONAL PREDISSOCIATION OF BENZENE DIMERS AND TRIMERS BY THE CROSSED LASER-MOLECULAR BEAM TECHNIQUE

M. F. Vernon,[a] J. M. Lisy,[b] H. S. Kwok,[c] D. J. Krajnovich,[a] A. Tramer,[d] Y. R. Shen[e] and Y. T. Lee,[a]

Materials and Molecular Research Division
Lawrence Berkeley Laboratory
University of California
Berkeley, California 94720

ABSTRACT

A molecular beam composed predominantly of benzene monomer, dimer, and trimer is excited with tunable, pulsed, infra-red radiation in the C-H stretch frequency range (3000-3100 cm^{-1}). Two types of experiments are performed for the observation of the vibrational predissociation of the excited cluster, measuring directly the wavelength dependence of the predissociation yield and the translational energy distribution of the predissociation products. The wavelength dependence of the vibrational predissociation is found to be similar to the infra-red spectra of room temperature liquid benzene. The translational energy distributions of the predissociation products are used to deduce dynamical properties for the following predissociation mechanism

---

a. Also associated with the Department of Chemistry, University of California, Berkeley.
b. National Science Foundation Postdoctoral Fellow, 1979-80.
c. Permanent Address: Department of Electrical Engineering, State University of New York, Buffalo, NY 14226.
d. Permanent Address: Laboratoire de Photophysique Moleculaire, Batiment 213, Universite de Paris-Sud, 91405 Orsay, France.
e. Also associated with the Department of Physics, University of California, Berkeley.

$$(C_6H_6)_n + h\nu \xrightarrow{\tau} (C_6H_6)_{n-1} + C_6H_6^{**}$$

where ** indicates vibrational excitation. The lifetime, τ, of the vibrationally excited clusters is determined to be in the range of $10^{-12} < \tau < 10^{-6}$ seconds. The most probable predissociation is characterized by all of the excess energy appearing in the rotational and vibrational motions of the products. The two product molecules do not seem to share this excess energy equally, the monomer product retaining in excess of 2/3 of the available energy. These observations are qualitatively consistent with current theories of vibrational predissociation of weakly bound molecular clusters.

INTRODUCTION

Since the observation by Welsh and McKellar of fine structure in the pressure induced infra-red spectra of H_2 with various gases (D_2, H_2, Ar, Kr, Xe, N_2, etc.) at low temperatures (1), van der Waals molecules have exhibited a number of intriguing properties which test our understanding of intermolecular forces. One property, in particular, which has been recently studied experimentally and theoretically is the vibrational predissociation lifetime of a van der Waals molecule when one of the vibrations of the strong chemical bonds is excited. This vibrational energy is typically 5-50 times the van der Waals bond energy. Early calculations by Child (2) on the lifetimes of Ar...HCl(v=1) suggested that the vibrationally excited complex was stable to dissociation for times comparable to the infra-red radiative lifetime. The spectra of McKellar and Welsh showed that for systems such as Ar...H_2(v=1), the lifetimes are sufficiently long to resolve rotational motions of the H_2 molecule within the complex.

In 1978 Scoles, Gough, and their coworkers (3) first observed directly the vibrational predissociation of a van der Waals molecule, $(N_2O)_2$, in the ground electronic state, obtaining a lifetime in the range $10^{-12} < \tau < 10^{-4}$ seconds. The clusters were excited by a diode laser and the predissociation observed as a decrease in signal at a bolometer which monitored the molecular beam. Since that time, the Waterloo group has studied CO_2 clusters using an F-center laser for excitation (4). Levy and coworkers have performed many experiments on

the vibrational predissociation of rare gas-iodine clusters in an excited electronic state (5). The predissociation was observed in the dispersed fluorescence spectrum of the I_2 fragment produced by the predissociation. Limits to the lifetimes could be determined from the absorption linewidths or by using competing I_2 electronic predissociation or fluorescence rates as an internal clock. From these results, a detailed picture of the propensity rules in vibrational predissociation has been obtained. In addition to earlier work in our laboratory on $(NH_3)_2$ (6), Reuss (7), Gentry (8) and Janda (9) and their coworkers have observed vibrational predissociation of various clusters with CW or pulsed CO_2 lasers and mass spectrometer detectors. In particular, Janda was able to argue convincingly from the observed linewidths and signal strengths that the predissociation was occurring on a timescale of 0.3 - 1.0 picoseconds for ethylene complexes. In a recent study of hydrogen bonded water clusters using a crossed laser-molecular beam apparatus and an optical parametric oscillator (10), it was demonstrated that vibrational excitation in the wavelength range 3000-3800 cm^{-1}, mainly associated with the O-H stretching motion, results in cluster predissociation. Furthermore, it was shown that the wavelength dependence of the predissociation signal is proportional to the photon absorption cross section. The variation of the spectra with cluster size gave valuable information on the hydrogen bond in water. Information on the internal energy distribution of the predissociation fragments and an upper bound for the predissociation time scale were also obtained.

Current experimental and theoretical studies have also used small clusters as simple model systems for learning about intermolecular interactions. For this reason, it is useful to have data for a wide range of compounds with different strengths of intermolecular forces to test the validity of cluster models under a variety of conditions.

Benzene is a natural choice due to its widespread use in simulations of liquid behavior (12,13,14) and the existence of a large body of spectroscopic data in different phases (15,16,17). Extensive modeling of the intermolecular potential function for benzene has been done by Evans and Watts (12) who have derived a six-centered Lennard-Jones potential which adequately describes the second virial coefficient, the static lattice energy, the solid state crystal structure, liquid phase distribution functions, viscosity, and thermal conductivity. Simpler models have been proposed by Lowden and Chandler (14) and MacRury, Steele, and Berne (13) and where comparison is possible, there is qualitative agreement on the interpretation of the results. For example, all have predicted that the local structure in the room temperature liquid should be similar to the solid with a preferred T-shaped nearest neighbor geometry.

In a molecular beam electric resonance study, Janda et al. (18) have shown that benzene dimer is polar, strongly suggesting that the gas phase dimer is also T-shaped. The similar near neighbor geometry in the dimer and condensed phases is the basis for assuming that a simple model for some condensed phase properties might be found in the small, gas phase clusters.

Two general theories have addressed the vibrational predissociation rate question - the "momentum gap" model of Ewing (19) and the "energy gap" model of Beswick and Jortner (20). The basic prediction of both theories is that the most efficient predissociation mechanism minimizes the translational energy of the predissociation products. The physical basis for this minimization of the tranlational energy was shown to be the poor overlap between the continuum translational wavefunction of the products and the initial "bound" state intermolecular wavefunction of the vibrationally excited cluster.

To date, these models have been applied only to binary complexes such as He...I_2 (21). A recent theoretical study of $(N_2O)_2$ by Ewing (22) is especially intriguing. According to the momentum gap model, Ewing predicted that the most probable dissociation channel involves a V→V,T energy transfer to the ν_1=1 vibrational state of the N_2O monomer when the ν_3=1 mode is excited. This product state minimizes the translational energy of the fragments. Using a realistic model function for the intermolecular potential, Ewing also concluded that a dipole-dipole coupling was more consistent with the dissociation lifetime than the Morse coupling of the intermolecular vibrational (and dissociation) coordinate. Beswick and Jortner, using a different dimer geometry and intermolecular potential, predict that the two N_2O monomer products will be left in the ν_2 = 1 and ν_1 = 1 states respectively (20). The energy gap and product states for this process is different than that predicted by Ewing. Therefore, the theoretical models are sensitive to details of both the intermolecular potential and the

physical mechanism which determines the predissociation lifetime. The simplicity of the Ewing and Beswick/Jortner models for a wide range of molecules invites further experimental confirmation. Using benzene as a "large molecule" test case to investigate cluster dissociation, other factors in intermolecular vibrational energy relaxation might be necessary to understand the product state distributions if more than one vibrational state has a small momentum gap (20).

EXPERIMENTAL

The two experimental methods described below utilize a supersonic expansion to prepare a spatially well defined molecular beam containing the benzene clusters, an infrared laser to excite the vibrational motions of interest, and a mass spectrometer to detect the effects on the clusters of laser excitation. One scheme is based on looking for the disapperance of clusters in the molecular beam correlated with the pulsed laser, similar to the method of Janda, et al. (9), while a second scheme monitors the appearance of molecular fragments created by the predissociation as in photofragment translational energy spectroscopy (11).

A. Infrared Laser

Tunable, infra-red radiation is generated by a Nd:YAG pumped optical parametric oscillator (OPO) based on the L-shaped cavity design of Byer, et al. (23). The far-field pumping arrangement, cavity design, and optics are shown in Fig. 1. The idler frequency easily tunes in the 3000-3100 cm^{-1} range corresponding to the C-H stretching motions in benzene. The repetition rate is 10 Hz, and the output power is 1-4 millijoules/pulse with 1 joule/cm^{-2} of Nd:YAG pump energy fluence. The OPO linewidth (the frequency difference between the half power points) in this wavelength range is measured to be 3-4 cm^{-1}. The duration of the OPO pulse is less than 10 nanoseconds.

B. Perpendicular Laser-Molecular Beam Arrangement

An in-plane view of this molecular beam configuration is shown in Fig. 2. In this arrangement, the vibrational predissociation process is observed by the detection of the predissociation products. The laser and molecular beams intersect at right angles, and a rotating mass spectrometer pivots about the intersection point. A series of defining slits restricts the acceptance angle of the mass spectrometer's ionizer to 2 degrees so that only those molecules whose velocities are oriented in the detector's direction and whose positions are within the acceptance cone can be detected. The background pressure in the intersection chamber is 1.0×10^{-7} torr, which ensures that all molecules which enter the detector from events in the intersection region are collision-free, primary products.

The molecular beam, produced by a supersonic expansion, is collimated by three apertures to an angular divergence of 1.5°. The nozzle temperature is 70°C. It was found that by bubbling He through room temperature benzene, the cluster distribution formed in the supersonic expansion could be controlled by simply changing the He pressure. The cluster distribution is measured by using the rotating mass spectrometer to directly sample the molecular beam.

The laser is coupled into the vacuum chamber by a BaF_2 lens held in a moveable tube which allows the OPO to be focused at the center of rotation of the detector where it intersects the molecular beam. An aperture in this tube spatially defines the laser beam diameter to a 2 mm

cross section at the intersection point. The laser is linearly polarized perpendicular to the plane defined by the laser and molecular beams. The output energy of the OPO idler frequency is measured with a germanium filter masked power meter placed a few inches after the intersection point. In this way, the power dependence of the absorption can be determined, and frequency variations in the photon number accounted for.

The signal produced by OPO photons is recovered from the background by gating a 255 channel, variable channel width, multichannel scaler (LBL 13X3381) with the laser pulse. The time delay between the OPO pulse and the arrival of molecules at the detector which were affected by the OPO photons is the sum of the neutral molecule flight time from the intersection region to the ionizer and the ion flight time through the quadrupole mass spectrometer to the ion counting electronics. The ion flight time is independently determined and subtracted prior to analysis.

C. Coaxial Laser-Molecular Beam Arrangement

A cross sectional view of this arrangement is shown in Fig. 3. In this configuration, the laser is colinear with the molecular beam. The electron bombardment ionizer and ion extraction optics are perpendicular to the laser and molecular beams. The quadrupole mass spectrometer directly monitors the molecular beam so the predissociation of clusters appears as a decrease in signal at the ion related to the predissociating parent clusters.

The signal is also gated by the laser and time resolved by the 255 channel multichannel scaler. The initial delay between the laser pulse and the onset of a change in the time resolved mass spectrometer signal is the sum of the ion flight time from the ionizer to the counting electronics and the flight time for the effects of the first cluster predissociations to reach the ionizer. The 65 cm flight path can detect lifetimes as long as 1.0 millisecond (for the nominal benzene molecular beam velocity of these experiments) while all lifetimes shorter than 1 microsecond (after correcting for the ion flight time) will appear to be "instantaneous". The power of the OPO is measured by monitoring a reflection of the OPO photons from a beam splitter.

RESULTS

From the experimental observations, two quantities are derived, the wavelength dependence of the predissociation cross sections and the translational energy distributions of the predissociation fragments. The photon energy is sufficient at the wavelengths 3000-3100 cm^{-1} corresponding to the benzene intramolecular stretching frequencies to break the weak intermolecular bond. The perpendicular molecular beam experiment uses the translational recoil velocity of the dissociated fragment clusters (which carries them away from the molecular beam) to detect the absorption of radiation. As shown in Fig. 4, the cluster predissociation fragments must have sufficient recoil energy to reach the detector when it is placed at a fixed angle relative to the molecular beam. Rotating the detector to successively larger angles favors those fragments which have higher translational energy. Through the energy balance equation

$$E'_{int} = E_{h\nu} + E_{int} - D_o - E'_t \qquad (1)$$

the internal energy in rotation and vibration of the fragments (E'_{int}) can be obtained from the photon energy ($E_{h\nu}$), the initial internal energy of the clusters (E_{int}), the dissociation energy (D_o) and the product recoil energy (E'_t) which can be derived from the measurements of laboratory angular and velocity distributions.

For the measured product yield at a fixed detector angle to be proportional to the photon absorption cross section of the parent

cluster, the time scale, τ, for the predissociation process must follow two restrictions. First, for the predissociation to be detected, the vibrationally excited clusters must not travel outside the detector's viewing region before dissociating. For the nominal benzene beam velocity, (1×10^5 cm/sec), this places an upper limit of 2 microseconds on τ. Secondly, τ cannot vary with the OPO wavelength in such a way as to produce a change in the shape of the laboratory angular distribution. Within the experimental statistical counting error, this has been verified for the systems reported here and the results are shown in Fig. 5. Changing the orientation of the laser polarization with respect to the detector-molecular beam plane had no effect on the signals.

The coaxial arrangement directly measures the depletion of the clusters and is not sensitive to the translational energy distribution. As such, it is free from any assumptions regarding the shape of the laboratory photofragment distributions, and is limited only by the upper bound on the lifetime given by the 65 cm flight path. It is to be pointed out, that in the colinear experiment, the signal is proportional to the number of polymers dissociating within 1 millisecond after excitation while in the perpendicular beam experiment only the fragments formed during the first 2 microseconds after the laser pulse may be detected. Both spectra being identical, we can assume that $\tau \leq 2$ microseconds for all wavelengths measured, and that the assumptions concerning the shape of the laboratory distributions in the perpendicular arrangement are valid.

In Fig. 6, the off axis predissociation spectra taken at the parent ions of benzene monomer (mass 78) and pentamer (mass 390) using the perpendicular laser-molecular beam configuration are shown. These signals represent the total laser induced signal corrected for background and photon number and, consequently, are proportional to the absorption cross section. These masses, to have reached the detector, must have originated from a cluster containing at least two or six benzene molecules respectively. Therefore, the spectra are labeled according to the smallest polymer capable of contributing to that mass, although fragmentation of larger clusters to these masses either in the predissociation process or by the electron bombardment ionization may also contribute. From Fig. 6, it can be concluded that the frequency shifts of the different polymers are small compared to the laser spectral bandwidth. The atypical beam conditions for these spectra, (Ar carrier gas and a room temperature nozzle), can produce large clusters. The principal spectral change is in the relative intensities of the three bands, showing that a unique spectral identification of the absorbing clusters is not possible at this resolution.

To assign the off-axis predissociation fragment signals to a parent cluster, the pressure dependence of the off-axis signals were compared to the pressure dependence of the polymers in the molecular beam, obtained by rotating the mass spectrometer to 0° along the molecular beam axis. In Fig. 7, the ratios of the off-axis predissociation fragment signals at mass 78 to the parent molecular beam mass 156 and 234 signals with the detector placed at 0° are plotted as a function of the nozzle stagnation

pressure. The 78 (off-axis fragments)/156 (0° molecular beam parent) ratio is flat, while the 78 (off-axis fragments)/234(0° molecular beam parent) ratio falls sharply. This is consistent with assuming that the off-axis mass 78 signal comes from the molecular beam cluster detected at 0° at mass 156, presumed to be the dimer. Under these expansion conditions, the signals in the molecular beam which relate to clusters containing more than three monomers are negligible. The ratios of mass 156:mass 234:mass 312 in the molecular beam are 100:3:0.3.

In a molecular beam study on the polarity of benzene polymers (18), it was concluded that only 1/10 of the benzene dimers were ionized to the parent mass peak. With this known proclivity for fragmentation of the neutral clusters by electron bombardment other evidence is necessary to show that the mass 78 off-axis signal is indeed that of the monomer photofragment from predissociation dimers, and not the ionization by-product of dimer photofragments originating from the predissociation of trimer and larger clusters. To verify these mass assignments, the coaxial laser-molecular beam configuration is used.

Figure 8 shows two time-resolved signals obtained with the coaxial method as well as a time-of-flight spectra obtained with the perpendicular method by placing the detector at zero degrees. This simulates the depletion scheme of the coaxial configuration. The increase in sensitivity is dramatic, a consequence of the increased interaction volume between the laser and molecular beams. From the decrease in signal at mass 78 in the coaxial arrangement, it is clear that the clusters are fragmented by electron impact to mass 78 ions.

That is, when the laser dissociates the benzene clusters, they are no longer present at the ionizer to fragment by electron bombardment to mass 78. The slight positive signal at mass 50 comes from the increase in the neutral monomer density resulting from the photodissociation of benzene clusters in or near the ionizer. Its shorter time duration is a result of the progressively smaller solid angle of acceptance for cluster photofragments more than a few centimeters from the ionizer. This different temporal behavior from the mass 78 signal shows that mass 50 ions correlate only to neutral benzene monomers. It also shows that the mass 78 signal cannot be explained as a change in the monomer fragmentation pattern which might occur should the monomer beam component be vibrationally excited by the laser. Since the mass spectra of benzene monomer has prominent peaks at mass 78 and 50-52 (24), one would expect the laser related signals at these masses to extend for a time equal to the neutral monomer flight time from the nozzle to the detector, if the monomer were absorbing radiation. The mass 50-52 signals are inconsistent with this explanation. The experimentally derived partial electron bombardment fragmentation pattern is summarized by

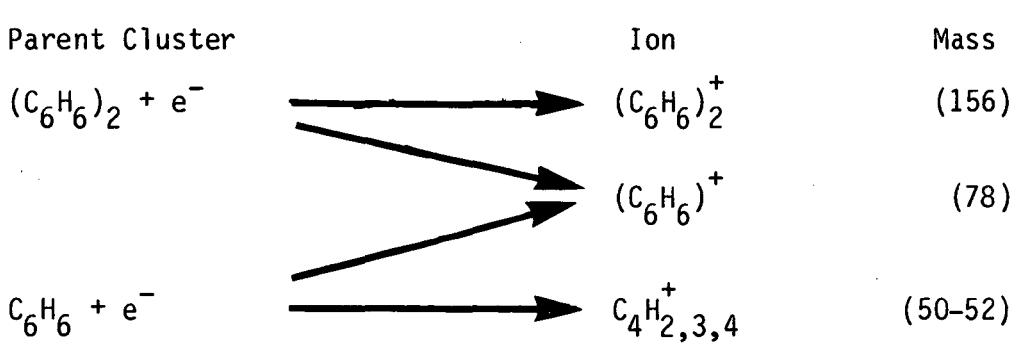

(2)

From the preceding analysis, it is clear that if the mass 50-52 angular scan in the perpendicular laser-molecular beam geometry is the same as the mass 78 scan, that the mass 78 data relates to benzene monomer predissociation fragments and not ionization fragments from higher clusters. Figure 9 shows the time of flight data taken at the two masses for two laboratory angles, establishing the validity of the previous assumption that the mass 78 off-axis signal results from ionizing monomers. The mass 156 off-axis signal is assigned to the trimer predissociation based on the strength of the observed signal, the tetramer and larger clusters in the molecular beam are present in negligible amounts.

The angular distributions of the mass 78 and 156 products, shown in Fig. 10, are similar in shape and extend only 10 degrees from the molecular beam. By measuring the beam velocity, V_b, of the initial clusters using a rotating slotted disk placed at a known distance from the ionizer (25), the transverse velocity of the predissociation fragments can be computed from the laboratory angle if the functional form of the center of mass angular distribution is known. The observed steep monotonic increase of the dissociation signal with decreasing laboratory angle can only be fit with a translational energy distribution which also has a similar decrease with increasing translational energy and peaks very near zero translational energy.

An analytical function of the form

$$P(E) = \alpha e^{-\alpha E} \qquad (3)$$

was used to quantitatively fit the measured laboratory angular and time-of-flight distributions. This center of mass energy distribution is convoluted over the experimental conditions (the finite aperture sizes, initial velocity distribution of the molecular beam, and ionizer length) assuming an isotropic center of mass angular distribution. The small range of laboratory angles where product is observed is insensitive to details of the center of mass angular distribution. Furthermore, it is shown below that it is reasonable to assume that the vibrationally excited complex rotates several times before predissociating. An isotropic center of mass distribution is appropriate in this case. In Fig. 10, the best fit curves for the mass 78 (α=5) and 156 (α=7) signals are compared with the experimental data.

From the measured wavelength dependence of the predissociation cross sections, it is clear that the perturbations of the three monomer vibrational bands in the 3000-3100 cm^{-1} range are small. The resolution of the laser is insufficient to observe rotational fine structure. No additional vibrational bands were observed which could be attributed to different bonding sites in the clusters or to a reduction of D_{6H} symmetry in the monomers. Combination bands involving intermolecular vibrations with an absorption strength greater than 5 of the fundamentals were not detected in this wavelength range. The absence of P, R rotational branches in the predissociation spectra limits the internal temperature of the clusters or the potential barrier hindering individual molecular rotation as in liquid, room temperature benzene.

The observed signals were all linear in photon number. Additional absorption of photons by the predissociation products was not observed at this photon flux (~7 x 10^{17} photons/cm^2).

DISCUSSION

From the results of these experiments, there are three properties of the vibrational predissociation which can be determined, the identification of the main product channels, the lifetime of the vibrationally excited clusters, and the internal energy distribution of the products.

The main product channels established by the pressure dependence and mass spectroscopy of the OPO induced signals for the predissociation of benzene dimers and trimers are

$$\begin{aligned} (C_6H_6)_2 + h\nu &\longrightarrow 2C_6H_6 \\ (C_6H_6)_3 + h\nu &\longrightarrow (C_6H_6)_2 + C_6H_6. \end{aligned} \qquad (4)$$

From the consistency of the wavelength dependence of the two predissociation signals measured in the perpendicular and coaxial configurations, it is clear that the clusters are predissociating within several microseconds of the laser pulse. A lower limit to the vibrationally excited state lifetime of 1 picosecond may be deduced by ascribing all of the observed linewidths (neglecting the ~3-4 cm^{-1} spectral bandwidth of the OPO and the initial internal state distribution of the clusters) to homogeneous broadening caused by the predissociation. This lower limit is consistent with the lack of a polarization dependence for the observed signals in the perpendicular configuration. If the rotational distribution of the dimers is

characterized by the same temperature as the molecular beam translational energy distribution (50°K) and can be modeled as a simple diatomic with 5 Å bond length, the most probable rotational state has a classical rotational frequency of 1 picosecond. A polarization dependence would be expected if the predissociation lifetime was significantly shorter than this rotational frequency <u>and</u> if the transition dipole has a fixed orientation with respect to the intermolecular axis. Since the intermolecular forces are poorly understood, large amplitude motion of the low frequency vibrations may well preclude such a fixed transition moment. Consequently, the lack of a polarization dependence is consistent with the lower lifetime limit deduced from the linewidth, but does not supply an independent determination of it. Recently, predissociation attributed to benzene dimers near 1040 cm^{-1} has been observed (26,27) with a linewidth of less than 3 cm^{-1} (26).

The translational energy distribution which adequately fits the data peaks at zero translational energy and has a very narrow energy spread. Therefore, the energy in internal excitation of the fragments for the most probable case is

$$E'_{int} = E_{int} + E_{h\nu} - D_o \qquad (5)$$

For simplicity, the initial internal energy is neglected. The adiabatic cooling in this nozzle expansion is expected to make this term small compared to the errors in the remaining larger contributions to the internal energy.

An estimate for the bond energy between two benzene molecules may be obtained from the crystal sublimation energy at 0°K. Model calculations (12,13) which reproduce this value give ~750 cm^{-1} for the pair potential zero point binding energy. Therefore, the internal energy of the fragments determined from equation 5 is 2300 cm^{-1}.

How is this energy distributed among the available internal states of the monomer and dimer fragments from the trimer predissociation? If all the excess energy were placed in the dimer fragment, it would be far in excess of the dimer bond energy and the dimer would be expected to predissociate before reaching the ionizer. The observation of dimer product then places a lower limit of 1550 cm^{-1} to the internal energy in the monomer. The rate of energy migration among the three benzene molecules in the trimer is then slower than the predissociation rate for this unequal energy distribution to be observed. Likewise, the photon excitation is to a particular monomer and that is the monomer which is vibrationally excited in the predissociation products, implying that the benzene monomers are located at distinguishable sites in the trimer. If this were not true, the zeroth order vibrational wavefunction would be delocalized over the three monomers.

One can tentatively generalize this conclusion to the case of dimers; we expect the dissociation to yield one "vibrationally hot" and one vibrationally cold molecule. This is consistent with the postulated T-shaped dimer structure where the two molecules are not equivalent.

The above predissociation mechanism qualitatively agrees with the momentum gap model proposed by Ewing. The substantial internal excitation of the products automatically reduces the momentum gap to a small value. The density of internal vibrational states near 2000 cm^{-1} in benzene monomer is sufficient to ensure that there will always be a resonant state within 10 cm^{-1} even if the rotational excitation is not significant. This high density of states is advantageous for testing in finer detail the predissociation process, because there are probably several states with nearly the same momentum gap. Other factors not explicitly considered in the momentum gap model to date, especially, the detailed predissociation dynamics, will have to be understood in order to predict the relative vibrational, rotational state populations in the products. Such state distributions are expected to become available in the near future for some of these systems from laboratory measurements. An accurate determination of the ground state binding energy can also be deduced from such measurements from the highest vibrational-rotational state populated in the products.

CONCLUSION

The crossed-laser molecular beam technique has been used to measure the absorption spectra and translational energy distributions of benzene dimers and trimers. The measured spectra are similar to the room temperature liquid. The weak perturbations in benzene were not expected to disturb the benzene monomer spectra, so no new spectroscopic information was derived from the absorption curves. The mechanism for the energy disposal was partially determined by the product angular distribution, which unequivocally establishes that the energy in excess of the intermolecular bond remains in internal vibrations or rotations of the fragments. The observation of the same behavior in both the dimer and trimer dissociation fragments further indicated this energy most probably remains in the monomer fragment which is originally excited. The time scale, τ, for the predissociation was limited to the range 1 picosecond $< \tau <$ 1 microsecond.

ACKNOWLEDGMENT

This work was supported by the Assistant Secretary for Nuclear Energy, Office of Advanced Systems and Nuclear Projects, Advanced Isotope Separation Division, U.S. Department of Energy under Contract No. W-7405-Eng-48.

REFERENCES

1. A. R. W. McKellar and H. L. Welsh, J. Chem. Phys. 61, 4636 (1974).

2. C. J. Ashton, Part II B.A. Thesis, Oxford University (1976) unpublished, M. S. Child, Faraday Discussions, Chem. Soc. 62, 307 (1977); C. J. Ashton, Ph.D. Thesis, Oxford University (1979).

3. T. E. Gough, R. E. Miller and G. Scoles, J. Chem. Phys. 69, 1588 (1978).

4. Infrared Laser Spectroscopy of Molecular Beams, Roger Miller, Ph.D. Thesis, University of Waterloo, Waterloo, Ontario (1980).

5. Donald Levy, Adv. Chem. Phys. XL VII, Part 2, p.323-362 (1981), Wiley and Sons.

6. A. Sudbo, P. A. Schulz, Y. T. Lee and Y. R. Shen, Proc. of the First International School on Laser Applications to Atoms, Molecules and Nuclear Physics, (Vilhuis, USSR, 1978).

7. "Laser Induced Predissociation of SF_6 Clusters", J. Geraedts, S. Setiadi, S. Stolte and J. Reuss, to be published.

8. W. R. Gentry, Mark A. Hoffbauer, Clayton F. Giese, VII International Symposium on Molecular Beams (Trento, 1979).

9. Michael P. Casassa, David S. Bomse, J. L. Beauchamp and Kenneth C. Janda, J. Chem. Phys. 72, 6805 (1980), ibid, 74, 5044 (1981).

10. "Infra-red Vibrational Predissociation Spectra of Water by the Crossed Laser-Molecular Beam Technique", M. F. Vernon, D. K. Krajnovich, H. S. Kwok, J. M. Lisy, Y. R. Shen and Y. T. Lee, to be published.

11. R. K. Sparks, L. R. Carlson, K. Shobatake, M. L. Kowalczyk and Y. T. Lee, J. Chem. Phys. 72, 1401 (1980).

12. (a) D. J. Evans and R. O. Watts, Mol. Phys. 29, 777 (1975); (b) ibid, 31, 83; (c) ibid, 32, 93.

13. T. B. MacRury, W. A. Steele, Bruce J. Berne, J. Chem. Phys. 64, 1288 (1976).

14. Lawrence J. Lowden, David Chandler, J. Chem. Phys. 61, 5228 (1974).

15. Paul C. Painter and Jack L. Koenis, Spectro. Acta 33A, 1003 (1977).

16. Peter Pulay, Geza Fogaraji, James Boggs, J. Chem. Phys. 74, 3999 (1981).

17. M. Spoliti, S. Nunziante Cesaro, V. Grosso, Spectro. Acta 32A, 145 (1976).

18. Kenneth Janda, John C. Hemminger, John J. Winn, Stewart E. Novick, Stephen J. Harris, and William Klemperer, J. Chem. Phs. 63, 1419 (1975).

19. Carlos Manzanares and George Ewing, J. Chem. Phys. 69, 1418 (1978).

20. J. A. Beswick and J. Jortner, Adv. Chem. Phys., XL VII, Part 2, p.363-506 (1981).

21. J. A. Beswick and G. Delgado-Burrio, J. Chem. Phys. 73, 3653 (1980); and J. A. Beswick, J. Jortner, Mol. Phys. 34, 1137 (1980).

22. Daniel A. Murales and George E. Ewing, Chem. Phys. 53, 141 (1980).

23. Stephen Brosnan and Robert Byer, IEEE Jour. Quant. Elect. QE-15, 415 (1979).

24. E. Stenhasen, S. Abrahamsson, F. McLafferty, Atlas of Mass Spectral Data, Vol. 1, Interscience 1969, 101. The ratios of mass 78:52:51:50 are 1000:177:157:126.

25. Kelvin rare gas time of flight program, Matthew Vernon, LBL Report 12422 (1981).

26. Kenneth Janda, private communication.

27. R. Gentry, unpublished results.

FIGURE CAPTIONS

Fig. 1. Schematic diagram of the Nd:YAG pumped OPO. Components indicated are: 1. Telescope, 2. Input coupler (100% transmittance at 1.06 μ, 100% reflectance at 1.4-2.1 μ), 3. Gold mirror, 4. 30°C temperature stabilized, angle tuned $LiNbO_3$ crystal, 5. Output coupler (100% transmittance at 1.06 μ, 50% reflectance at 1.4-2.1 μ), 6. Double pass YAG mirror (100% reflectance at 1.06 μ, 100% transmittance at 1.4-4.0 μ), 7. BaF_2 lens.

Fig. 2. In plane view of perpendicular laser molecular beam apparatus. Labeled components are: 1. 0.007" quartz nozzle heated to 70°C, 2. First skimmer, 3. Second skimmer, 4. Third skimmer, 5. Power meter, 6. Germanium filter, 7. Ionizer assembly. 8. Quadrupole mass spectrometer. θ measures the angle of rotation of the detector from the molecular beam.

Fig. 3. Side view of the coaxial laser-molecular beam apparatus. Labeled components are: 1. BaF_2 entrance window for the OPO beam, 2. Quadrupole mass spectrometer, 3. Ionizer assembly, 4. Final molecular beam defining aperture, 5. Second skimmer, 6. First skimmer, 7. Nozzle.

Fig. 4. Schematic view of the perpendicular arrangement showing how the recoil velocity of the predissociation fragment relates to the detector's laboratory angle, θ, relative to the molecular beam. The insert shows that the angle is determined from the

vector addition of the recoil velocity (dotted arrows) and the initial beam velocity (thick arrow). The final laboratory velocities are the solid arrows, also shown at the intersection point of the OPO and molecular beams.

Fig. 5. Wavelength dependence of the mass 78 angular distributions. Open circles ν_{OPO} = 3040 cm^{-1}, solid circles, ν_{OPO} = 3095 cm^{-1}. The 3040 cm^{-1} data have been displaced +0.5° relative to the 3095 cm^{-1} data to allow easier comparison.

Fig. 6. Wavelength dependence of the predissociation cross sections. A) Mass 390, $(C_6H_6)_5^+$, at 400 torr Ar with T_{nozzle} = 25°C, B) Mass 78, $C_6H_6^+$, at 250 torr Ar with T_{nozzle} = 25°C.

Fig. 7. Pressure dependence of the mass 78 signal in the perpendicular arrangement with the detector angle at θ = 4 . The solid points are the ratio mass 78(θ = 4)/mass 156(θ = 0), the open circles are the ratio mass 78(θ = 4)/mass 234(θ = 0).

Fig. 8. Comparison of the time resolved mass spectrometer signals of the perpendicular and colinear configurations. A) Mass 78 data taken at θ = 0 in the perpendicular laser-molecular beam arrangement, B), C), D) are masses 156, 78, and 50 respectively of the colinear configuration.

Fig. 9. Time of flight spectra at masses 78 (solid points) and 50 (open circles). A) Detector angle θ = 4 , B) Detector angle θ = 5 .

Fig. 10. Angular distribution of predissociation fragments. Solid points are mass 156, open circles are mass 78. The curves are the calculated distributions using the center of mass energy distribution given by Eqn. 3. For mass 78 and 156, the best fit values for α are 5 and 7 respectively.

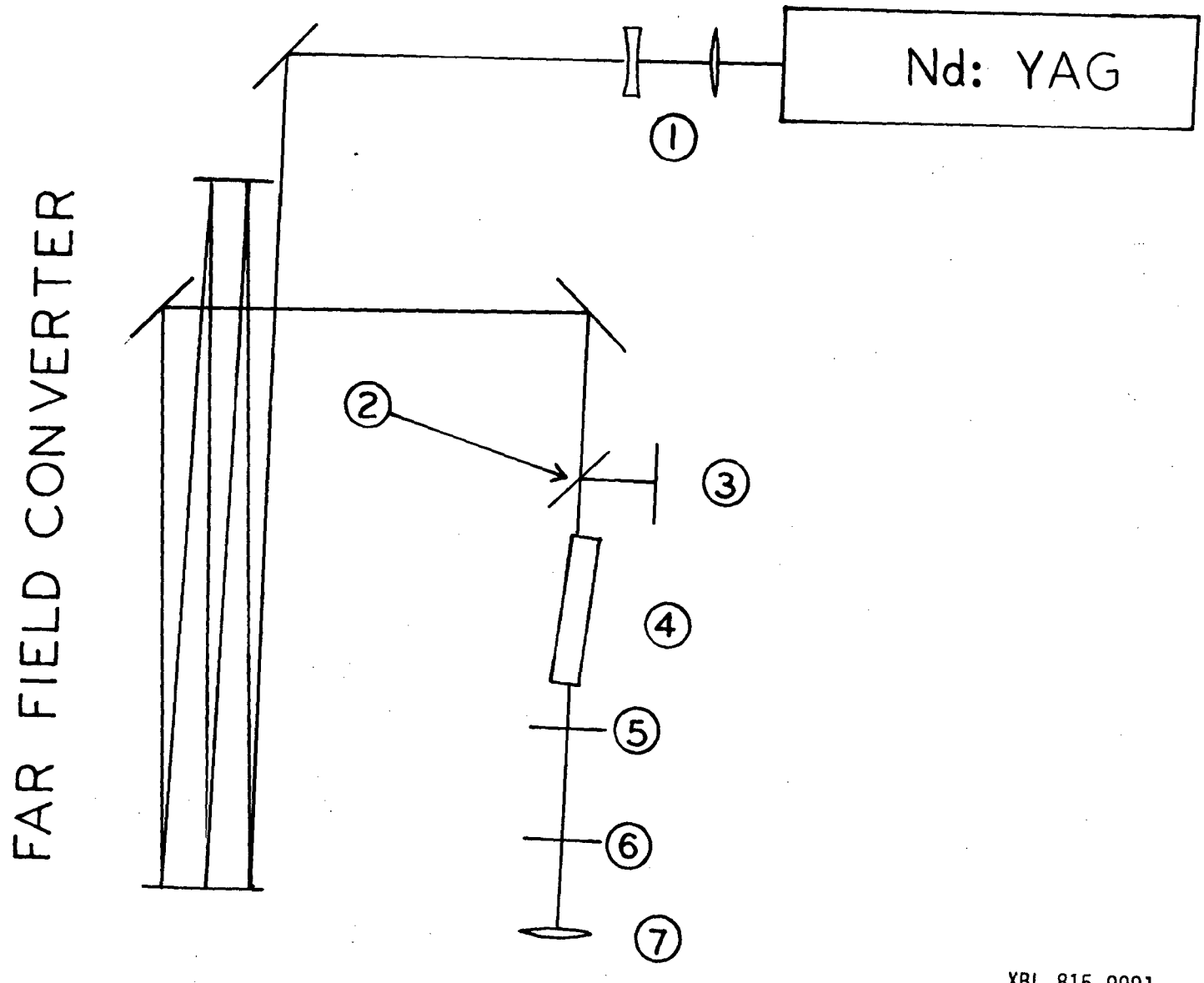

Fig. 1

XBL 815-9991

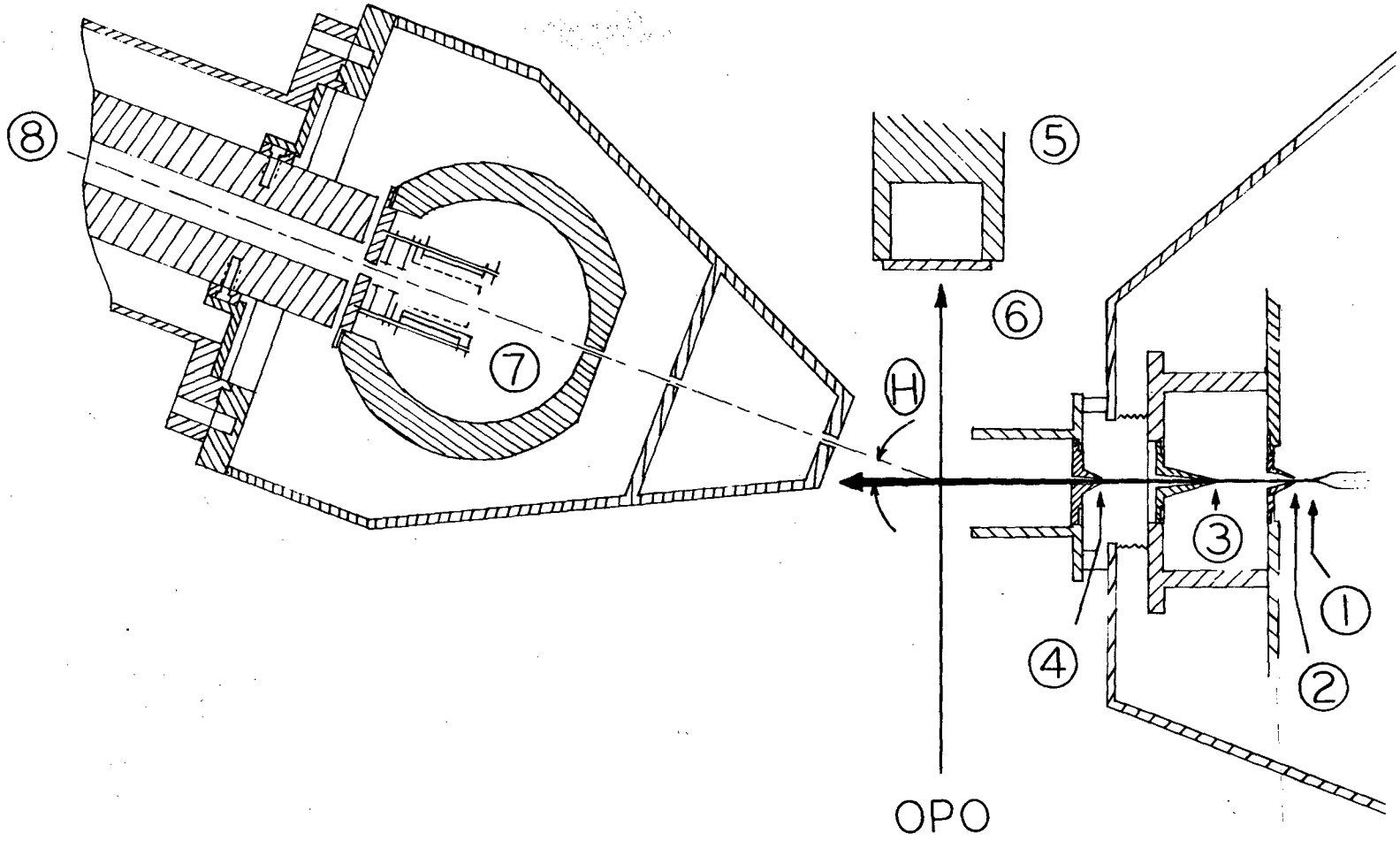

Fig. 2

XBL 815-9930

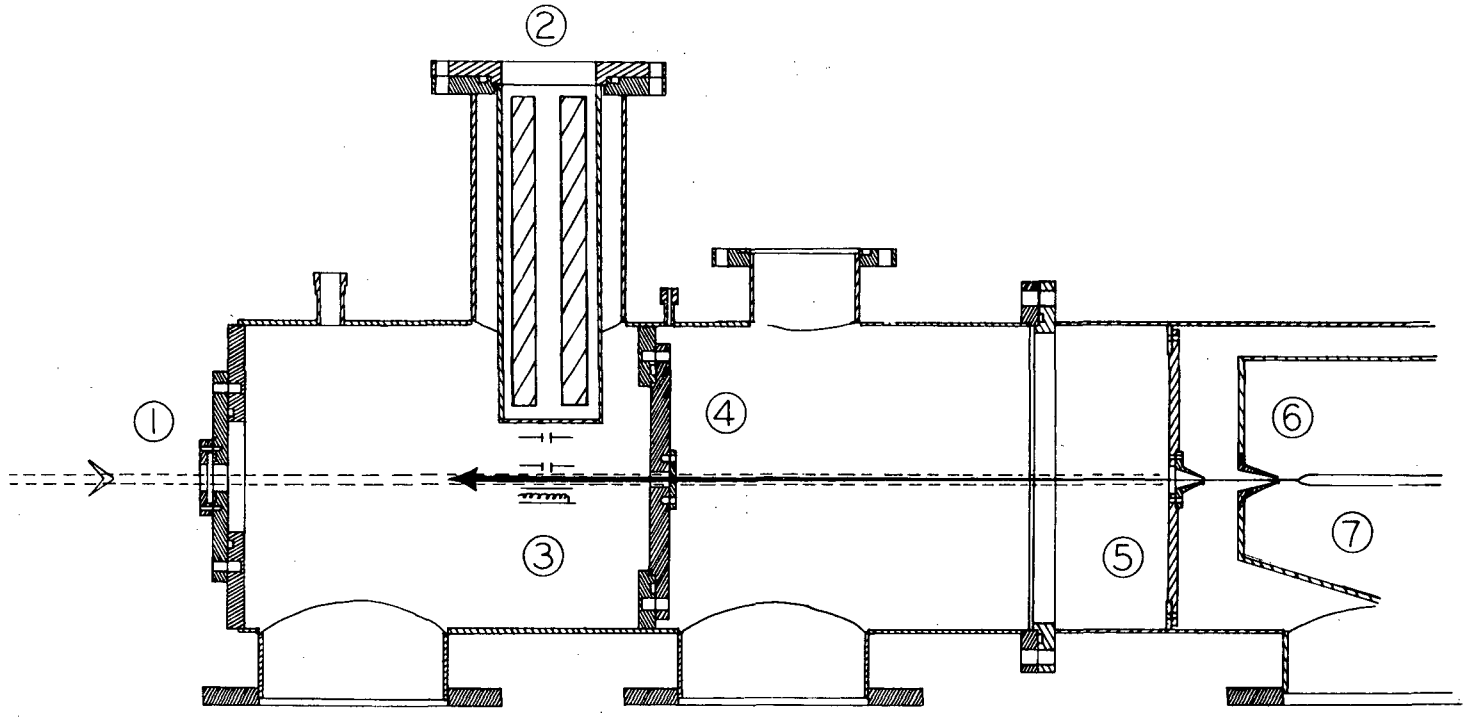

XBL 815-9994

Fig. 3

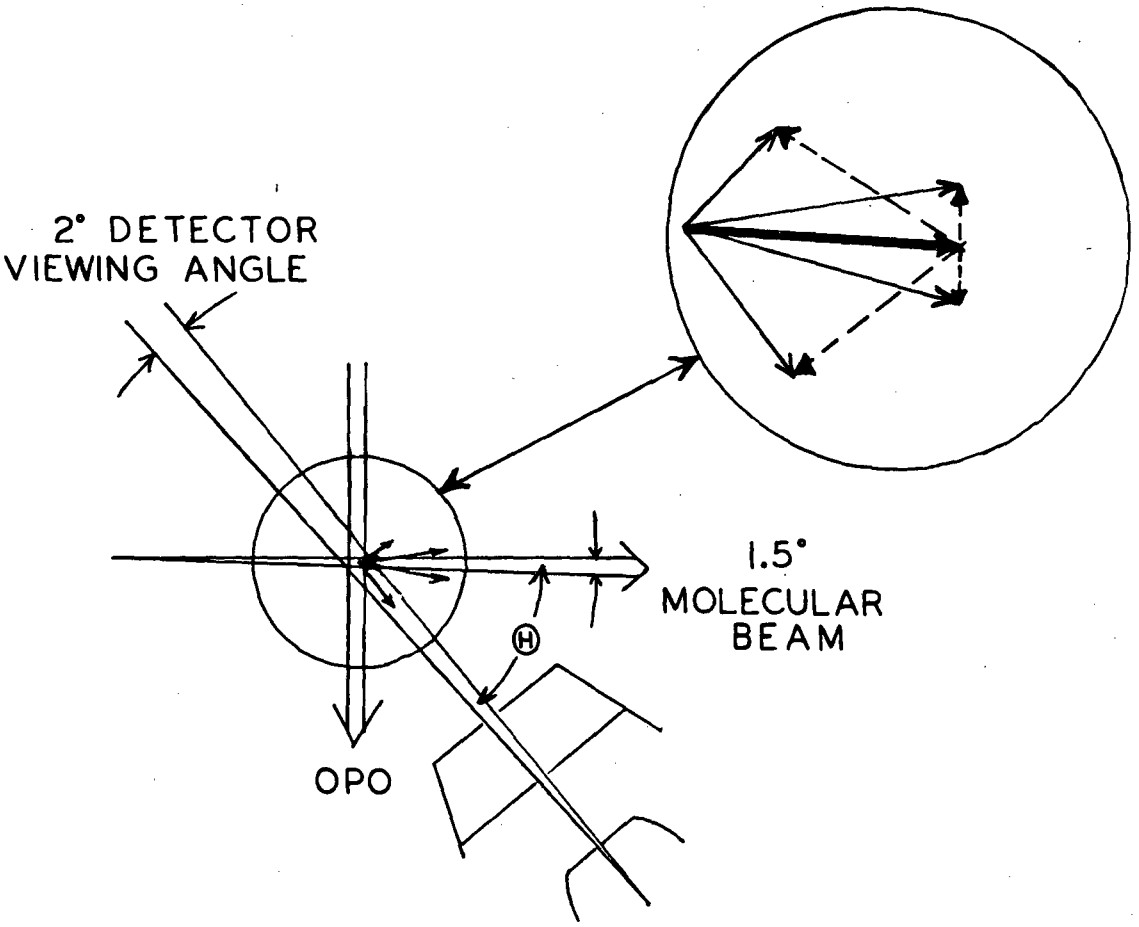

XBL 816-9998

Fig. 4

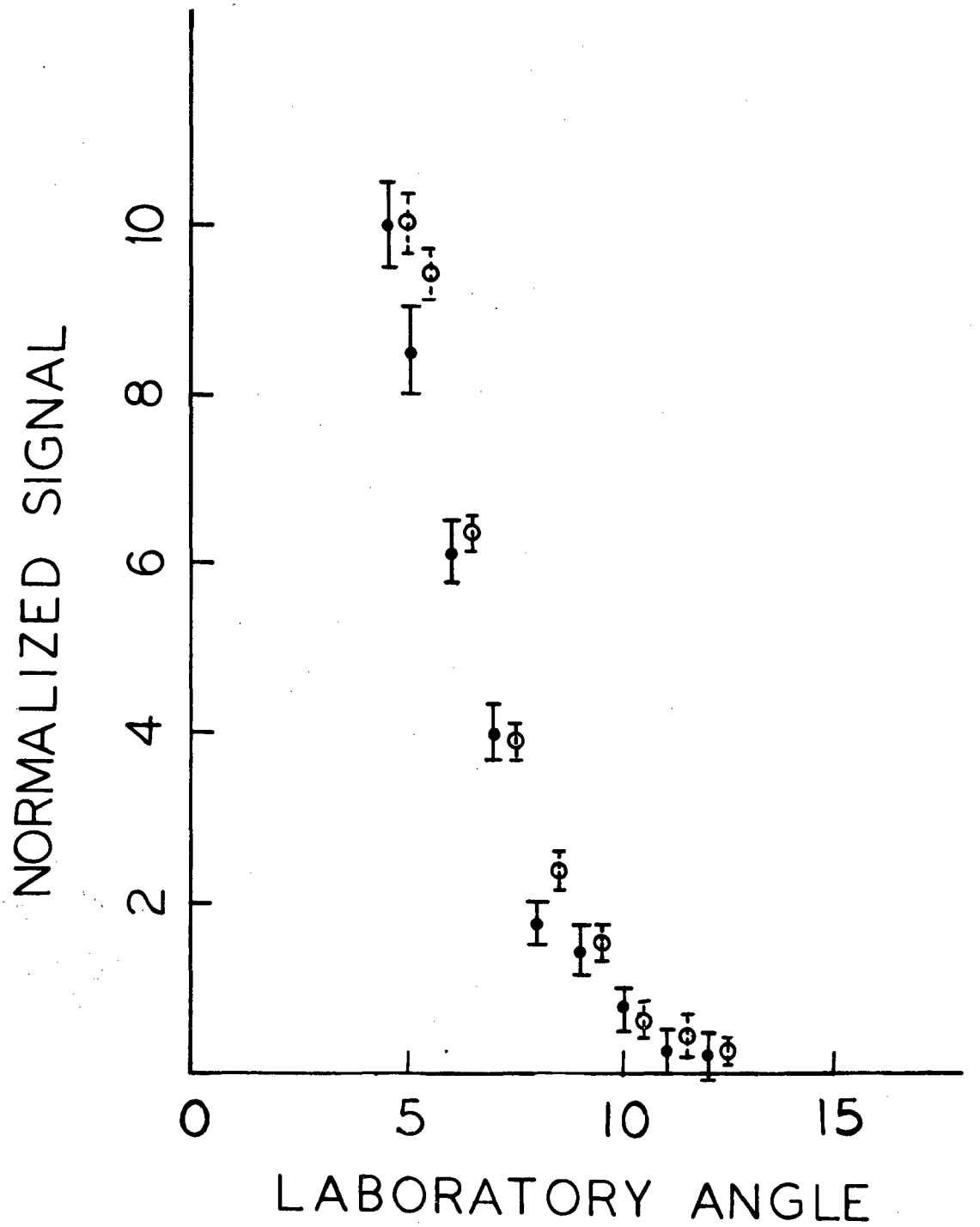

XBL 816-9996

Fig. 5

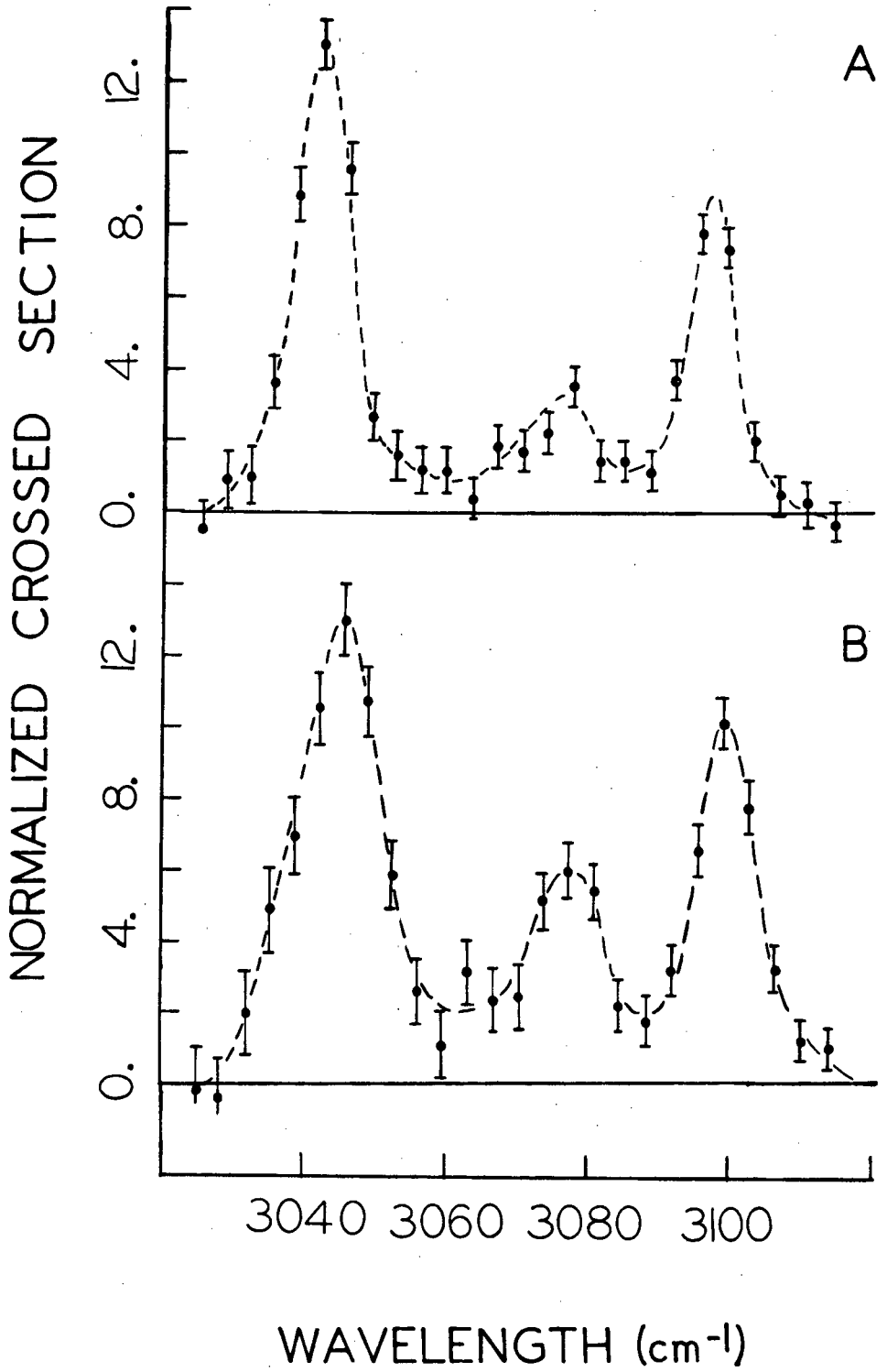

XBL 815-9992

Fig. 6

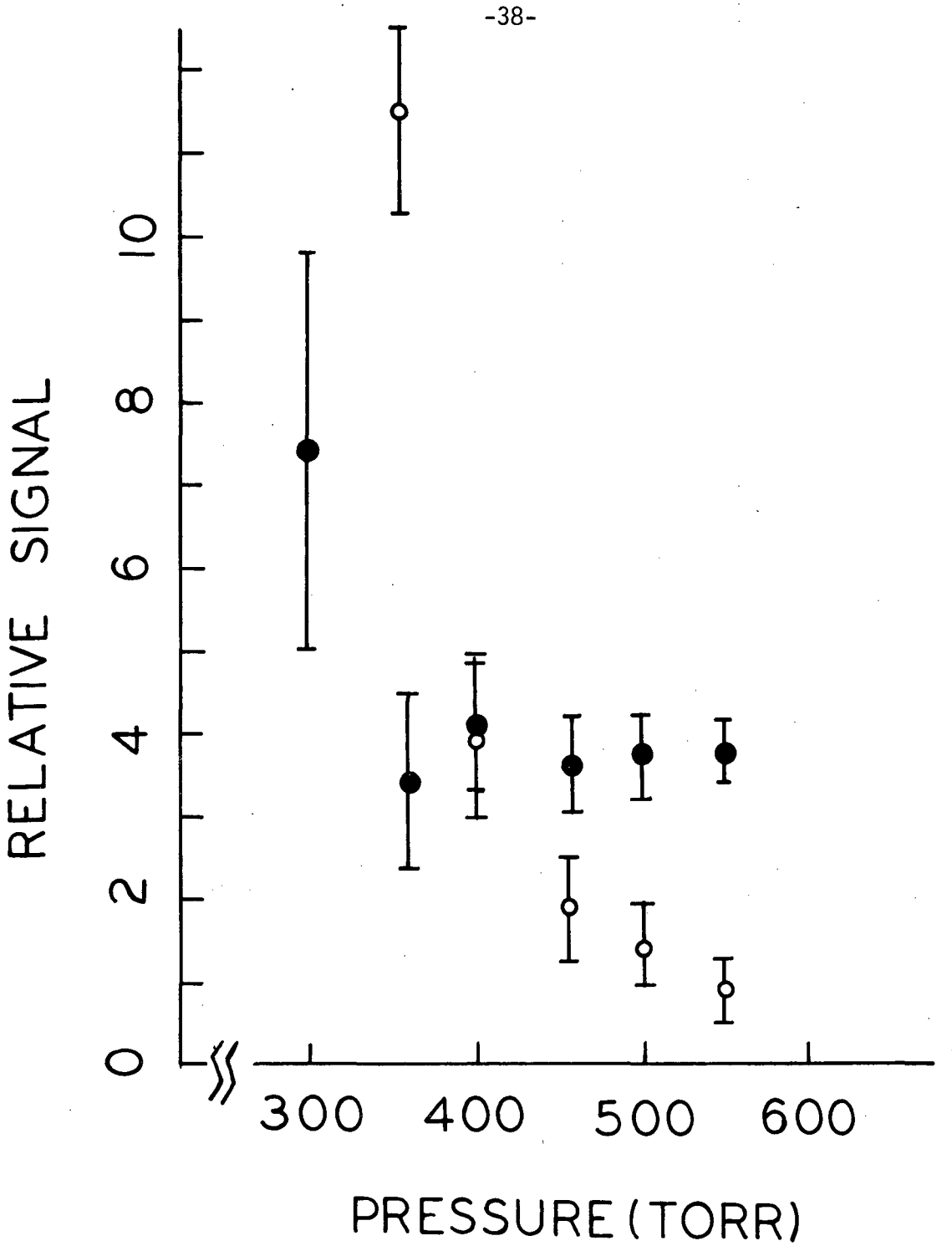

XBL 816-9997

Fig. 7

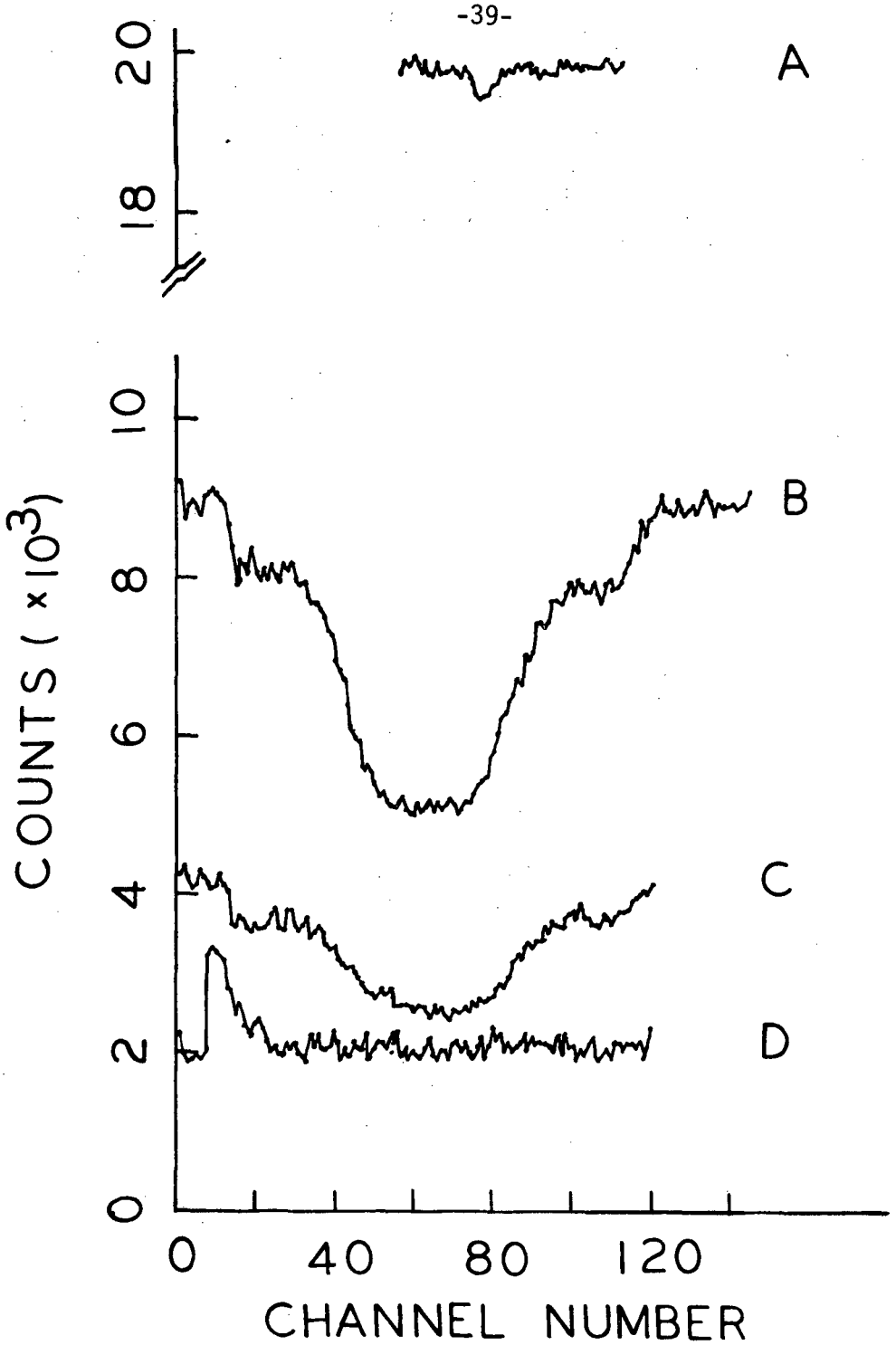

Fig. 8 XBL 815-9989

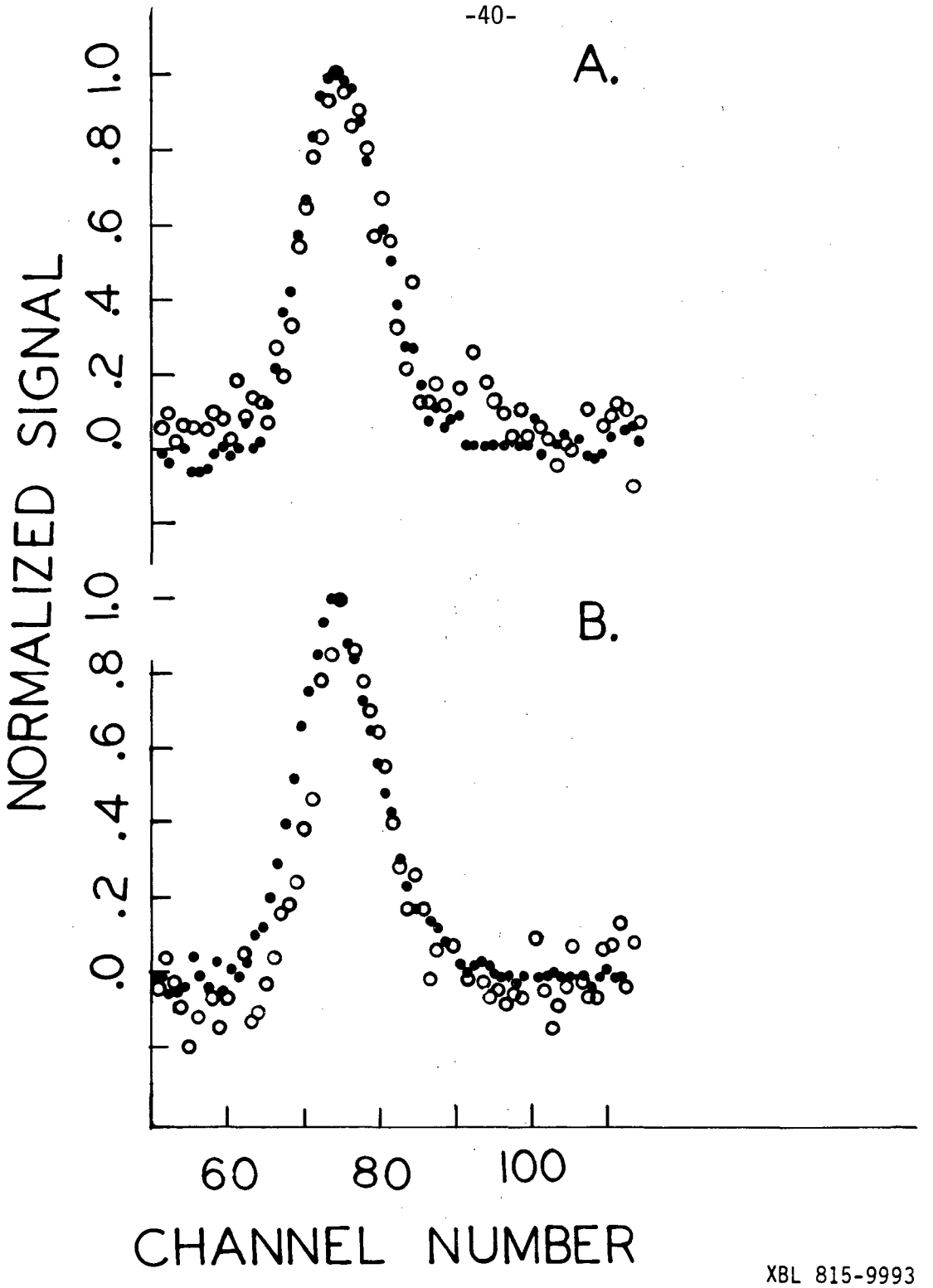

XBL 815-9993

Fig. 9

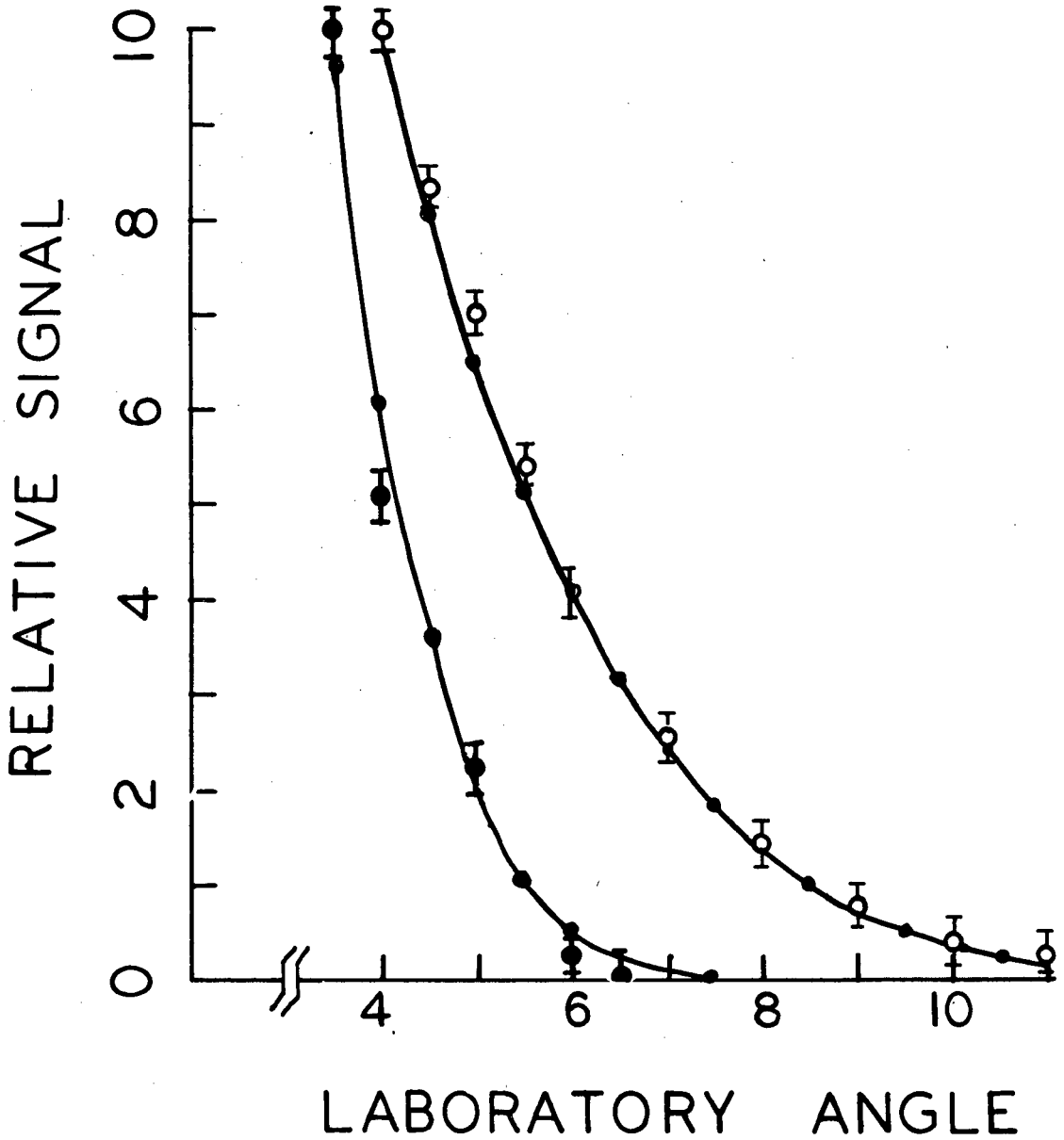

Fig. 10

XBL 816-9995

This report was done with support from the Department of Energy. Any conclusions or opinions expressed in this report represent solely those of the author(s) and not necessarily those of The Regents of the University of California, the Lawrence Berkeley Laboratory or the Department of Energy.

Reference to a company or product name does not imply approval or recommendation of the product by the University of California or the U.S. Department of Energy to the exclusion of others that may be suitable.

TECHNICAL INFORMATION DEPARTMENT
LAWRENCE BERKELEY LABORATORY
UNIVERSITY OF CALIFORNIA
BERKELEY, CALIFORNIA 94720